Development of a device to stretch tissue-like materials and to measure their mechanical properties with scanning probe microscopy

Takeomi Mizutani*, Hisashi Haga, Kazushige Kawabata

Division of Biological Sciences, Graduate School of Science, Hokkaido University, North 10 West 8, Kita-ku, Sapporo 060-0810, JAPAN

*Corresponding author. Tel: +81 11 706 3810; Fax: +81 11 706 4992.

E-mail address: mizutani@sci.hokudai.ac.jp (T. Mizutani).

Abstract

We developed a new stretch device to investigate the biomechanical responses to an external loading force on a tissue-like material consisting of cells and a collagen gel. Collagen gel, a typical matrix found abundantly in the connective tissue, was attached to an elastic chamber that was precoated with a thin layer of collagen. Madin-Darby canine kidney (MDCK) cells that were cultured on the collagen gel were stretched in a uniaxial direction via deformation of the elastic chamber. Changes in the morphology and stiffness of the tissue-like structure were measured before and after the stretch by using wide-range scanning probe microscopy (WR-SPM). The change in cellular morphology was heterogeneous, and there was a 2-fold increase in the intercellular junction due to the stretch. In addition to the SPM measurements, this device enables observation of the spatial distribution of cytoskeletal proteins such as vimentin and α-catenin by using immunofluorescent microscopy. We concluded that the stretch device we have reported in this paper is useful to measure the mechanical response of a tissue-like material over a range of cell sizes when exposed to an external loading force.

Keywords: scanning probe microscopy, collagen gel, stiffness, external loading force, epithelial cell

1. Introduction

An external loading force has crucial effects on the functions and structure of tissues. For example, bones require an external loading force to maintain their mechanical resistance; additionally, muscles and tendons need an external loading force to conserve their mechanical strength [1]. The external loading force is transmitted into the tissues in a heterogeneous manner based on the structure and mechanical properties of the tissue; therefore, the response of each region in the tissue to the external loading force is spatially different. The heterogeneity in the transmission of the external loading force into the tissue is essential for the maintenance of the tissue structure [2, 3]. However, it is difficult to examine the biomechanical effects of the external loading force on the tissues because there is no apparatus that can measure the local surface strain and local stiffness simultaneously.

The cellular contractile force also plays an important role in maintaining the tissue structure and functions by providing them with mechanical support. For example, this force is involved in physiological processes such as cellular migration [4], proliferation [5], and differentiation [6]. The activities of these physiological processes are strongly influenced by external loading forces [7-9]. However, the relationship between the external loading force and cellular mechanics remains unclear. Previously, we measured the changes in cellular stiffness in stretched or uniaxially-compressed fibroblasts cultured on an elastic substrate by using

mechanical-scanning probe microscopy (M-SPM) [10]; these changes corresponded with the contractile force of the stress fibers but not with the tension on the membrane. Thus, we concluded that the contractile force of a single fibroblast is maintained constant against an external loading force. The next issue that will be addressed by our current study is the mechanism by which the cellular contractile force responds to the external loading force in a tissue-like material comprising cells and the extracellular matrix (ECM).

We modified the M-SPM to enable visualization of topography and local stiffness in living cells in order to investigate the cellular stiffness and mechanical response of the cells toward external loading force using force mapping mode under liquid conditions [10, 11]. In order to measure the mechanical properties of a tissue-like material under an external loading force, we developed wide-range scanning probe microscopy (WR-SPM), which is a modification of a commercial M-SPM [12]. Using WR-SPM, we successfully observed the morphology and stiffness distribution of a large epithelial colony at a subcellular resolution. Thus, the local stress and strain of a tissue-like sample that is subjected to an external loading force can be measured by using WR-SPM.

The purpose of this study was to develop a new stretching device and investigate the local stiffness responses of a tissue-like material under an external loading force over a range of cell sizes (greater than 100 μm). A colony of Madin-Darby canine kidney (MDCK) cells was

cultured on a collagen matrix gel, which is a typical matrix found abundantly in the connective tissues; the colony was stretched in a uniaxial direction via the deformation of the elastic substrate to which the collagen gel was attached. Under this condition, the changes in the morphology and stiffness of the MDCK cells were measured using WR-SPM. In this paper, we discuss the effects of an external loading force on changes in the cellular and collagen stiffness and describe the impact of these changes on cellular physiology.

2. Materials and methods

2.1 Cell culture

Madin-Darby canine kidney (MDCK) cells were purchased from RIKEN BioResource Center (Tsukuba, Japan), and were cultured in low glucose DMEM (Invitrogen, Carlsbad, CA) containing 10% heat-inactivated fetal bovine serum (FBS) and 1% antibiotics (Invitrogen) in 5% CO_2 at 37 ^{o}C. The cells within the 10th passage were used for the WR-SPM measurements.

2.2 Stretch device and sample preparation

In order to subject the cells and the collagen gel to an external loading force, we developed a stretch device. This device is based on an equipment that we had previously developed [10]. It consists of an elastic chamber (Scholertec Corp, Osaka, Japan), a custom made clamping device, and a collagen matrix gel (Cellmatrix I-A; Nitta Gelatin, Osaka, Japan). The elastic chamber has a transparent bottom (20 × 20 mm) that is 200-μm thick, and it has a 5-mm high wall; this wall could be deformed up to 20% of the original cellular dimension along the uniaxial direction by using the handmade clamping device. Figure 1 shows the schematics of the sample preparation. In order to deform the collagen gel by stretching the chamber, it is necessary to ensure that the surface of the chamber is firmly attached to the collagen gel. Therefore, the chamber surface was precoated with a thin layer of collagen by air drying 0.3

mg/ml collagen solution (Cellmatrix I-C; Nitta Gelatin) diluted with 1 mM HCl (Wako Pure Chem., Osaka, Japan). Subsequently, the coated chamber was washed 3 times with PBS (Invitrogen) to remove the HCl. Collagen gelation was performed on the surface of the chamber at 37 ^{o}C according to a previously described method [13]. The concentration of the collagen was 1.2 mg/ml. The thickness of the collagen gel ranged from 40 to 70 μm. Subsequently, trypsinized epithelial cells were plated on the collagen gel on the chamber. The density of the cells was set at approximately 3×10^2 cells/mm^2. After a 24-h incubation, the culture medium was substituted with HEPES buffer containing low glucose DMEM and FBS (pH 7.2~7.3) to avoid the extreme fluctuation in the pH during the WR-SPM measurements.

2.3 Topography and stiffness measurements by WR-SPM

We used a commercially available 320-μm-long silicon-nitride cantilever with a spring constant of 0.01 N/m (MLCT-AUNM; Veeco, Woodbury, NY, USA). The topography and spatial distribution of stiffness were imaged using the conventional contact mode and the force mapping mode, respectively. The details regarding the measurement of stiffness have been described previously [14]. Briefly, the measurement provides topography and stiffness distribution simultaneously by tracing the surface of a target area and collecting a force-distance curve at each pixel point on the target area. The local stiffness (Young's modulus) of the

samples was evaluated quantitatively by using the Levenberg-Marquardt method [15, 16] fitting the data to the Hertzian contact model for a conical indentor [14, 17]. In this model, the loading force and indentation are related to the following equation.

$$F = \frac{\pi E \tan(\alpha)}{2(1-\nu^2)}\delta^2, \quad (1)$$

where F is the loading force, E and ν are the Young's modulus and Poison ratio of the sample respectively, α is the opening angle of the cone (= 35^o), δ is indentation into the sample. For simplification, ν was assumed as 0.5 in our studies.

The cells do not exactly fulfill the criteria for the Hertzian contact model because major components of the cells are viscoelastic and not isotropic. However, this assumption is likely to be adequate for a large number of applications, in which absolute elasticity values are not required [18, 19]. The effect of cellular viscosity on stiffness has been discussed previously [20]. In order to minimize the effect of cellular viscosity on the stiffness measurements, the indentation speed of the cantilever was set at 4 Hz according to a previous report [20].

2.4 Analysis of the strain fields

In order to analyze the stretch-induced strain fields on the collagen gels and the cells as a first approximation, we applied the following procedure. The characteristic features on the cell-gel complex were used as strain tracking marker, and these features in a set of unstretched

and stretched topographies were manually numbered. One of these structures was defined as the origin of this stretch analysis (in Fig. 2, the number 12 was defined as the origin). A line perpendicular to the direction of the stretch including the origin was drawn on the topographies (in Fig. 2, dashed line). We measured the distance from the line to each structure by using the Image-Pro Plus (Media Cybernetics, MD). The strain at a point was calculated by the following equation:

$$\varepsilon = \frac{l - l_0}{l}, \tag{2}$$

where ε is strain, l and l_0 are the distance from the line after and before stretch, respectively.

There are two possible effectors for the strain. The above analysis takes into account the strains between a pair of topography measurements. The strains were be mainly caused by the external stretch. However, some strains may be caused by changes in the cellular contractile force that is known to alter the local morphology of the collagen gel occasionally (e.g., Fig. 6). From this viewpoint, the current analysis is a first approximation of a strain field by a pure external stretch.

2.5 Immunofluorescence by a confocal microscope

We followed a previously described procedure to observe immunofluorescence [11]. Briefly, the cells were rinsed with PBS, followed by fixation with 4% formaldehyde/PBS for 10

min, washed again with PBS, and permeabilized with 0.5% Triton X-100/PBS for 10 min. Subsequently, the cells were stained with both specific primary antibodies/PBS and secondary antibodies/PBS for 1 h. A primary antibody that reacts with α-catenin was purchased from Zymed Laboratories (Carlton Court, SF). Alexa Fluor 546-labeled anti-mouse IgG (Invitrogen) was the secondary antibody that was used to detect the primary antibody, and Alexa Fluor 488-labeled phalloidin (Invitrogen) and Cy3-conjugated anti-vimentin (Sigma-Aldrich, St. Louis, MO) were used to stain filamentous actin and vimentin, respectively. Fluorescence images were obtained by using a confocal laser scanning microscope (C1 confocal imaging system; NIKON Instech, Kanagawa, Japan). Sectional images were collected and processed using the EZ-C1 software (NIKON Instech).

3. Results

In order to examine the mechanism by which the sample cells and collagen gel were stretched by the device, we measured the morphological changes in the cells and collagen gel during the uniaxial stretch using WR-SPM (Fig. 2) and analyzed the strain field (Table 1). Some areas of the collagen gel were observed to be homogeneously stretched; the distance between two arbitrary points was increased by 5% in the direction shown by the arrows in Figure 2. On the contrary, each cell was heterogeneously stretched; the variance of the increments ranged from 4% to 6%. These results indicate that the stretch device was able to produce local strains over a range of cell sizes under an external loading force.

In order to investigate the changes in cellular stiffness in the cells, we measured the stiffness map of the collagen gel and the cells before (Fig. 3(a)) and after the stretch (Fig. 3(b)). During the two stiffness map measurements, 15 min elapsed due to set up the sample position. Cellular stiffness at intercellular junctions and in other regions of the cells was averaged, and the change in stiffness—before and after the stretch—was compared (Fig. 3(c)). The number of data used for the statistical analysis was about 100 points in each condition. The junctional site showed a 2-fold increase in the stiffness. On the other hand, the stiffness of another region of the cell increased slightly. The typical force versus distance curves are shown in Figure 3(d). Both data matched well with the analytical curve. To quantify the changes in stiffness, local

stiffness of each image was plotted as a histogram, and the frequency of stiffness was fitted to a Gaussian function (Fig. 4). The stiffness of the collagen gel did not change under the stretch conditions. On the contrary, the stiffness of the cells increased under these conditions.

In order to test whether the stretch device can be used for light micrography with a high magnification, we performed immunofluorescence for filamentous actin, vimentin, and α-catenin after application of the stretch. The fine spatial distribution of each protein was obtained (Fig. 5). Filamentous actin was organized into thick bundles; vimentin formed slack networks; and α-catenin localized at the junctional sites. These findings were in agreement with previous reports.

Cells exhibit not only immediate responses within some seconds but also slow responses more than 10 min after being subjected to the external loading force [21, 22]. We investigated the changes in physiological activities of the cells in the stretch device for 1 h. We performed a time-lapse experiment to observe the morphology of the cells cultured on a collagen gel by using WR-SPM (Fig. 6). The colony consisted of approximately 20 cells, and the collagen fibers were orientated perpendicular to the peripheral cells of the colony. Further, the cells deformed a cleaved area on the gel and reoriented the collagen fibers in 1 h. The deformation and reorientation of the substrates indicate that the stretch device enables examination of cellular activities on a gel substrate during time-lapse measurements by using

WR-SPM.

4. Discussion

We succeeded in measuring the changes in the local stiffness in an epithelial colony under uniaxial stretch conditions by using a stretch device. Previously, Brown et al. had developed a stretch device that enables the measurement of the mechanical effects of an external loading force on a collagen gel in which the fibroblasts were embedded [23]. Our device differed from theirs in its ability to measure either gross or local stiffness in tissue-like materials. Our stretch device is useful in the investigation of local surface strain and local stiffness with a cellular range of tissues.

However, the temporal resolution of the stretch device is not good. In fact, it took 30 min to record a stiffness image. Our method cannot be used to observe cellular responses that are completed within a few seconds; for example, the dynamics of stress fiber response to external compression. Costa et al. showed that the stress fibers buckled at approximately 20% of cellular compression, disassembled in 5 sec, and reassembled within 60 sec [24]. In order to discuss such a rapid phenomena from the viewpoint of cellular mechanics, more high-frequency measurements of cellular viscoelasticity should be made available.

There are two possible reasons for the stretch-induced changes in the stiffness of the cells. First, it may be due to an elastic response of the actin filaments [25]; second, it may be attributed to the changes in the cellular activities such as enhancement of the contractile force

and reinforcement of stress fibers [10, 26]. Janmey et al. investigated the elastic property of an actin matrigel and showed that more than 10% of the strain was required to yield a 2-fold increase in stress [27]. In this study, the degree of the strain in the cells ranged from 4% to 6% (Fig. 2). Considering these findings, the degree of cellular deformation induced in this study was too small to yield a 2-fold increase in the stiffness of the actin networks. Therefore, the increase in the stiffness may be due to the physiological activities of the epithelial cells.

To our knowledge, the increased stiffness at the intracellular junctions of epithelial cells under stretch conditions (Fig. 3) has not been reported as yet. Trapet et al. stretched the epithelial cells and measured the viscoelastic moduli of the epithelial sheet [28]. They showed that cellular storage modulus increased with stretch. However, they did not report an increased stiffness at the intercellular junction. The physiological implications of increased stiffness at intercellular junctions are not yet known; however, we speculate that this increase would be involved in strengthening the intercellular adhesions to resist an external loading such as mechanical stretch. We intend to prove this hypothesis in our future studies by observing recruitment of intercellular adhesion proteins such as cadherins and catenins to the intercellular junctions under the mechanical stretch.

The stress on the collagen gel would relax within approximately 10 minutes. Approximately 20 min after the stretch, only 5% of the strain on the collagen gel actually

existed (table 1). The stiffness of the collagen gel areas did not change under the stretch conditions (Fig. 4). These results implied that the stress-relaxation was completed within 20 min. Shirazi et al. simulated that stress on collagen fibrils reduced for a minute [29]. Our suggestion was supported by their work except for the time scale of stress-relaxation. In order to agree with time-scale of stress relaxation, we will shorten the time between the measurements.

In future, we aim to study the types of physiological activities that are involved in the stiffness response under an external loading force since the present results indicate that the reinforcement of stress fibers and/or enhancement of the contractile force probably occur under the external loading force. In addition to the time lapse measurement of stiffness, observation of the tempo-spatial changes in the green fluorescent protein (GFP)-tagged actin filaments in stress fibers [10], measurement of tempo-spatial variations in Ca^{2+} [30], and measurement of the local activity of small GTPase RhoA by fluorescent resonance energy transfer (FRET) [31] are useful techniques to investigate the involvement of physiological activities in the stiffness response. We will employ these techniques by using our stretch device.

5. Conclusion

In this study, we showed that our stretch device was useful to explore the local stiffness responses under an external loading force in tissues. Using MDCK cells as an example, we investigated the cellular stiffness response to an external loading force. The stiffness at intercellular junctions increased under the external loading force. We speculated that the increase was due to the reinforcement of stress fibers or enhancement of the cellular contractile force. However, the molecular mechanisms involved in this response remain unclear. Further, we aim to elucidate the involvement of stress fiber reconstruction or actomyosin regulators in the stiffness responses under an external loading force.

Acknowledgement

We are grateful to the editor (Prof. William R. Wagner) and the reviewers for their helpful comments and advices. This work was supported by the Sasakawa Scientific Research Grant from The Japan Science Society, by the Naito Foundation, and by a Grant-in-Aid from the Ministry of Education, Culture, Sports, Science and Technology of Japan (14GS0301 for K. K.).

References

[1] Kjaer M. Role of extracellular matrix in adaptation of tendon and skeletal muscle to mechanical loading. Physiol Rev 2004;84(2):649-98.

[2] Wiskott HW, Belser UC. Lack of integration of smooth titanium surfaces: a working hypothesis based on strains generated in the surrounding bone. Clin Oral Implants Res 1999;10(6):429-44.

[3] van Eijden TM, Koolstra JH, Brugman P. Three-dimensional structure of the human temporalis muscle. Anat Rec 1996;246(4):565-72.

[4] Zelenka PS. Regulation of cell adhesion and migration in lens development. Int J Dev Biol 2004;48(8-9):857-65.

[5] Murthy K, Wadsworth P. Myosin-II-dependent localization and dynamics of F-actin during

cytokinesis. Curr Biol 2005;15(8):724-31.

[6] Engler AJ, Griffin MA, Sen S, Bonnemann CG, Sweeney HL, Discher DE. Myotubes differentiate optimally on substrates with tissue-like stiffness: pathological implications for soft or stiff microenvironments. J Cell Biol 2004;166(6):877-87.

[7] Li S. Analysis of endothelial cell migration under flow. Methods Mol Biol 2005;294):107-21.

[8] Cogoli A, Cogoli-Greuter M. Activation and proliferation of lymphocytes and other mammalian cells in microgravity. Adv Space Biol Med 1997;6):33-79.

[9] Searby ND, Steele CR, Globus RK. Influence of increased mechanical loading by hypergravity on the microtubule cytoskeleton and prostaglandin E2 release in primary osteoblasts. Am J Physiol Cell Physiol 2005;289(1):C148-58.

[10] Mizutani T, Haga H, Kawabata K. Cellular stiffness response to external deformation: tensional homeostasis in a single fibroblast. Cell Motil Cytoskeleton 2004;59(4):242-8.

[11] Nagayama M, Haga H, Takahashi M, Saitoh T, Kawabata K. Contribution of cellular contractility to spatial and temporal variations in cellular stiffness. Exp Cell Res 2004;300(2):396-405.

[12] Mizutani T, Haga H, Nemoto K, Kawabata K. Wide-range scanning probe microscopy for visualizing biomaterials in the submillimeter range. Jpn J Appl Phys 2004;43(7B):4525-28.

[13] Haga H, Irahara C, Kobayashi R, Nakagaki T, Kawabata K. Collective movement of epithelial cells on a collagen gel substrate. Biophys J 2005;88(3):2250-6.

[14] Haga H, Sasaki S, Kawabata K, Ito E, Ushiki T, Sambongi T. Elasticity mapping of living fibroblasts by AFM and immunofluorescence observation of the cytoskeleton. Ultramicroscopy 2000;82(1-4):253-58.

[15] Levenberg K. A method for the solution of certain problems in least squares. Quarterly J. Appl. Math. 1944;2):164-8.

[16] Marquardt D. An algorithm for least-squares estimation of nonlinear parameters. SIAM J. Appl. Math. 1963;11):431-41.

[17] Hertz H. On the contact of elastic solids. J. Reine Angew. Math. 1881;92):156-71.

[18] Matzke R, Jacobson K, Radmacher M. Direct, high-resolution measurement of furrow stiffening during division of adherent cells. Nat Cell Biol 2001;3(6):607-10.

[19] A-Hassan E, Heinz WF, Antonik MD, D'Costa NP, Nageswaran S, Schoenenberger CA, Hoh JH. Relative microelastic mapping of living cells by atomic force microscopy. Biophys J 1998;74(3):1564-78.

[20] Radmacher M, Fritz M, Kacher CM, Cleveland JP, Hansma PK. Measuring the viscoelastic properties of human platelets with the atomic force microscope. Biophys J 1996;70(1):556-67.

[21] Naruse K, Yamada T, Sokabe M. Involvement of SA channels in orienting response of cultured endothelial cells to cyclic stretch. Am J Physiol 1998;274(5 Pt 2):H1532-8.

[22] Wojciak-Stothard B, Ridley AJ. Shear stress-induced endothelial cell polarization is mediated by Rho and Rac but not Cdc42 or PI 3-kinases. J Cell Biol 2003;161(2):429-39.

[23] Brown RA, Prajapati R, McGrouther DA, Yannas IV, Eastwood M. Tensional homeostasis in dermal fibroblasts: mechanical responses to mechanical loading in three-dimensional substrates. J Cell Physiol 1998;175(3):323-32.

[24] Costa KD, Hucker WJ, Yin FC. Buckling of actin stress fibers: a new wrinkle in the cytoskeletal tapestry. Cell Motil Cytoskeleton 2002;52(4):266-74.

[25] Kojima H, Ishijima A, Yanagida T. Direct measurement of stiffness of single actin filaments with and without tropomyosin by in *vitro* nanomanipulation. Proc Natl Acad Sci U S A 1994;91(26):12962-6.

[26] Glogauer M, Arora P, Chou D, Janmey PA, Downey GP, McCulloch CA. The role of

actin-binding protein 280 in integrin-dependent mechanoprotection. J Biol Chem 1998;273(3):1689-98.

[27] Janmey PA, Euteneuer U, Traub P, Schliwa M. Viscoelastic Properties of Vimentin Compared with Other Filamentous Biopolymer Networks. Journal of Cell Biology 1991;113(1):155-60.

[28] Trepat X, Grabulosa M, Puig F, Maksym GN, Navajas D, Farre R. Viscoelasticity of human alveolar epithelial cells subjected to stretch. Am J Physiol Lung Cell Mol Physiol 2004;287(5):L1025-34.

[29] Shirazi R, Shirazi-Adl A. Analysis of articular cartilage as a composite using nonlinear membrane elements for collagen fibrils. Med Eng Phys 2005;27(10):827-35.

[30] Klepeis VE, Cornell-Bell A, Trinkaus-Randall V. Growth factors but not gap junctions play a role in injury-induced Ca^{2+} waves in epithelial cells. J Cell Sci 2001;114:4185-95.

[31] Yoshizaki H, Ohba Y, Parrini MC, Dulyaninova NG, Bresnick AR, Mochizuki N, Matsuda M. Cell type-specific regulation of RhoA activity during cytokinesis. J Biol Chem 2004;279(43):44756-62.

Figure legends

Figure 1

Procedure of sample preparation and SPM measurements. A sterilized elastic chamber was coated with a collagen solution diluted with HCl prior to overlaying a collagen gel. Epithelial cells were cultured on the collagen gel. The cells were stretched uniaxially during the SPM measurements.

Figure 2

Change in the topographic images of epithelial cells cultured on a collagen gel exposed to uniaxial stretch. The cells on the surface of the collagen gel were measured by SPM before (a) and after (b) the stretch. The direction of the uniaxial stretch was represented by a set of arrows. The length of the bar represents 50 μm. Some points on the image were numbered to analyze strain fields (c). The dashed line was defined as origin of the stretch.

Figure 3

Change in spatial stiffness due to the stretch. Epithelial cells cultured on a collagen gel were stretched and stiffness maps were measured before (a) and after (b) the stretch. The arrows indicate the direction of application of stretch. The bar represents 50 μm. The stiffness at

junctional sites and other regions of the cells was averaged and statistical changes in the averaged stiffness were examined using Student's *t* test (c). These data were presented as mean ± SEM from about 100 pixel points of each image (*$P < 0.05$). At the intercellular junction (indicated by an asterisk), a set of force versus indentation data was measured before (open circle) and after (open square) the stretch (d). Each data set was fitted to the Hertzian contact model, where the Hertzian curves in each data set are shown as a dotted line (before the stretch) and a solid line (after the stretch). We then obtained the stiffness of one of the parameters of each curve. The stiffness at the junctional site changed after the stretch (from 10 to 23 kPa).

Figure 4

Histograms of stiffness distribution of collagen gels and cells are shown in Fig. 3 (a and b). Each data was fitted to a Gaussian function.

Figure 5

Immunofluorescent micrographs of cytoskeletons and intercellular junctions. Epithelial cells on collagen gels were stretched by 5% and were then fixed and stained with phalloidin (a, c), anti-vimentin (b) or anti-catenin (d). Arrows indicate the direction of the stretch. The bar represents 50 μm.

Figure 6

Time-lapse images of the topography of epithelial cells on a collagen gel as measured by SPM. During the observation, the cells moderately deformed the collagen gel. The number in each image indicates the time lapsed (minutes) from the beginning οφ τηε οβσερωατιον. Α χλεαωεδ αρεα ον τηε γελ ατ 0 μιν (αν ελλιπσοιδ δοττε δ λινε) ωασ ρεοριεντεδ ωιτηιν 60 μιν (αν ελλιπσοιδ σολιδ λινε). Σομε χολλαγεν φιβριλσ (ινδιχατεδ βψ αν αρροω) ωερε δεφορμεδ βψ τηε χελλσ (ινδιχατεδ βψ αν αρροωηεαδ). Τ ηε λενγτη οφ τηε βαρ ρεπρεσεντσ 30 μm.

Strain fields on the collagen gel and the epithelial cells analyzed from Fig. 2

	Places in Fig. 2(c)	Strain (%)	
cells			
	1	4.5	
	2	5.2	
	3	6.3	
	4	5.7	
	5	6.2	
	6	4.8	
	7	5.2	
	8	6.8	
collagen gel			
	9	5.3	
	10	4.8	
	11	5.1	
	12	0	(defined as the origin of the stretch)
	13	5.5	
	14	4.7	
	15	5.2	
	16	5.4	
	17	4.8	

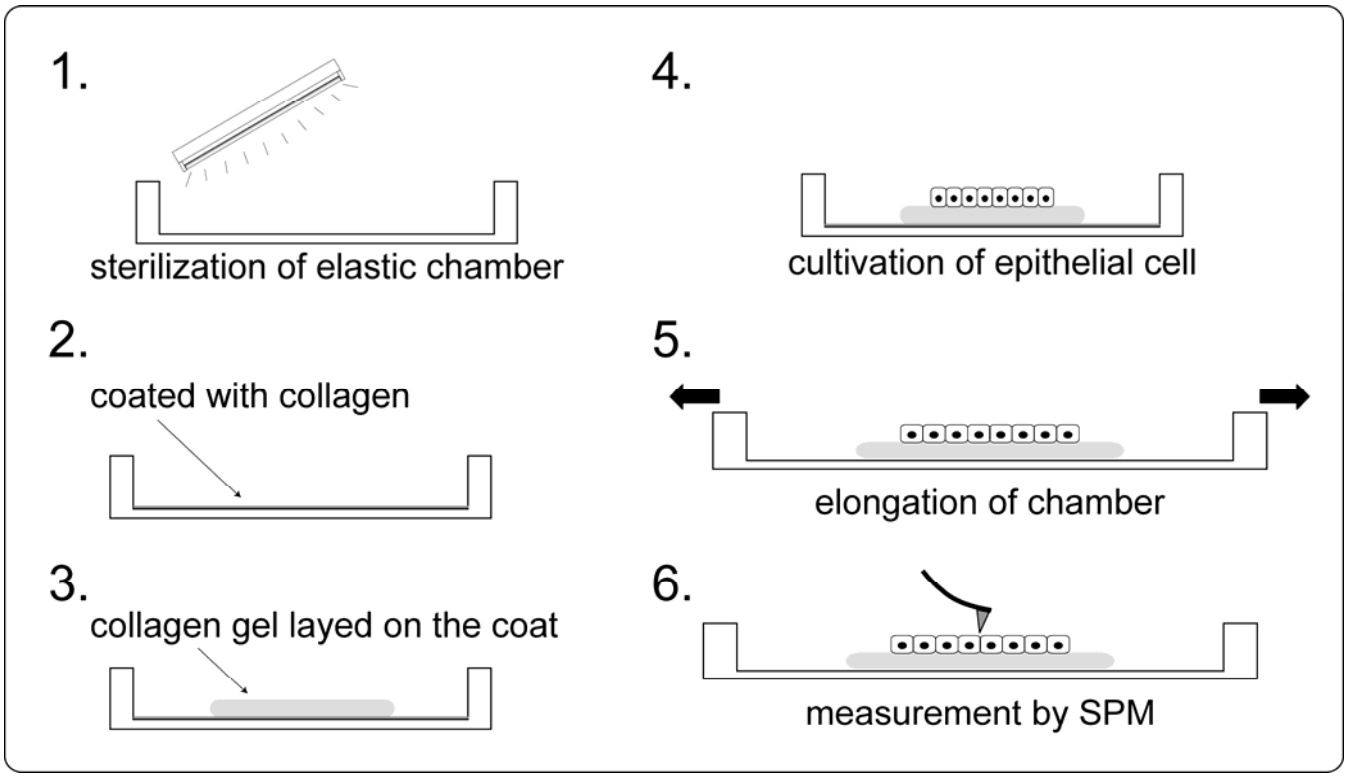

Figure 1

Width = 17.7 cm

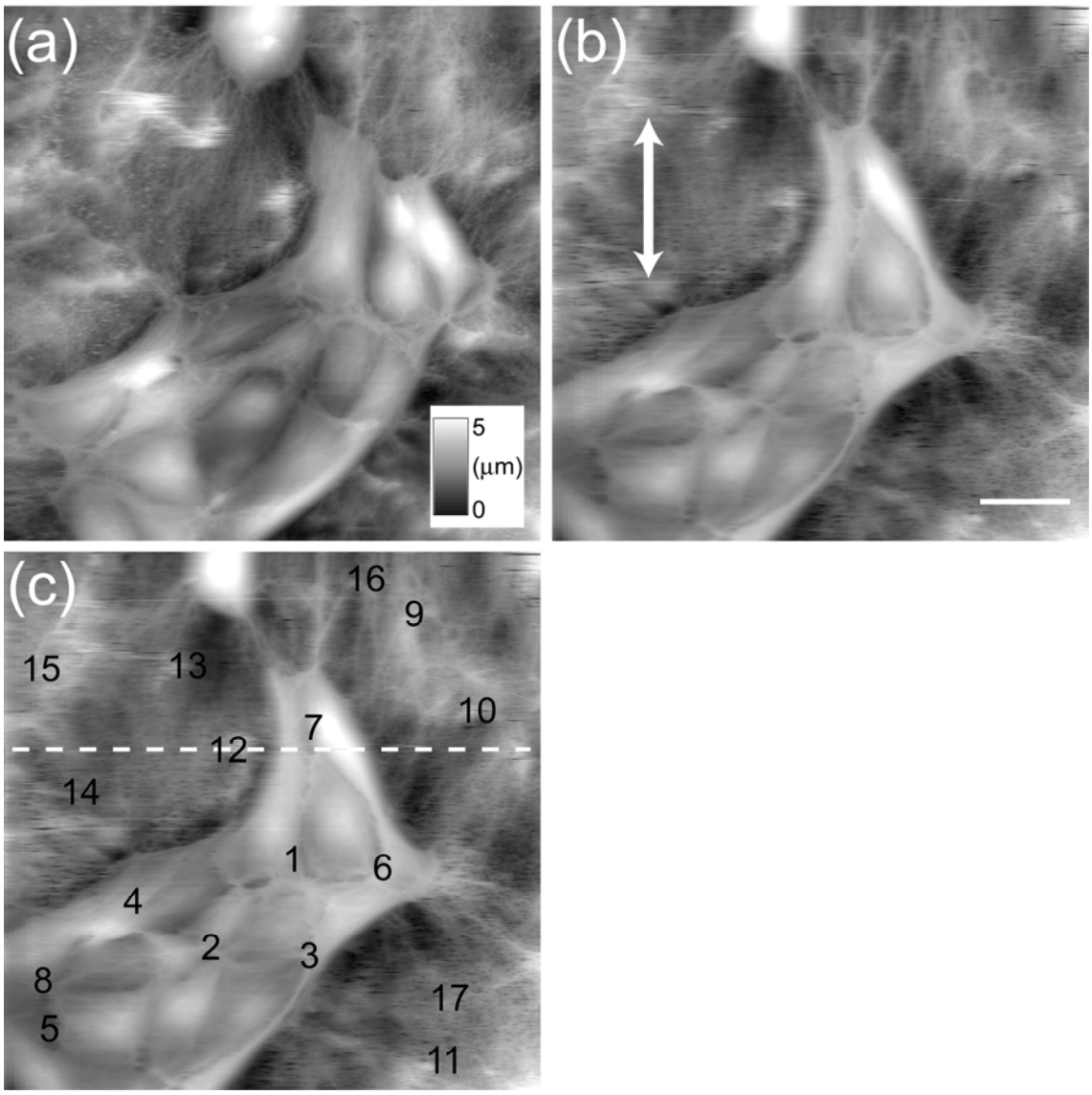

Figure 2

Width = 17.7 cm

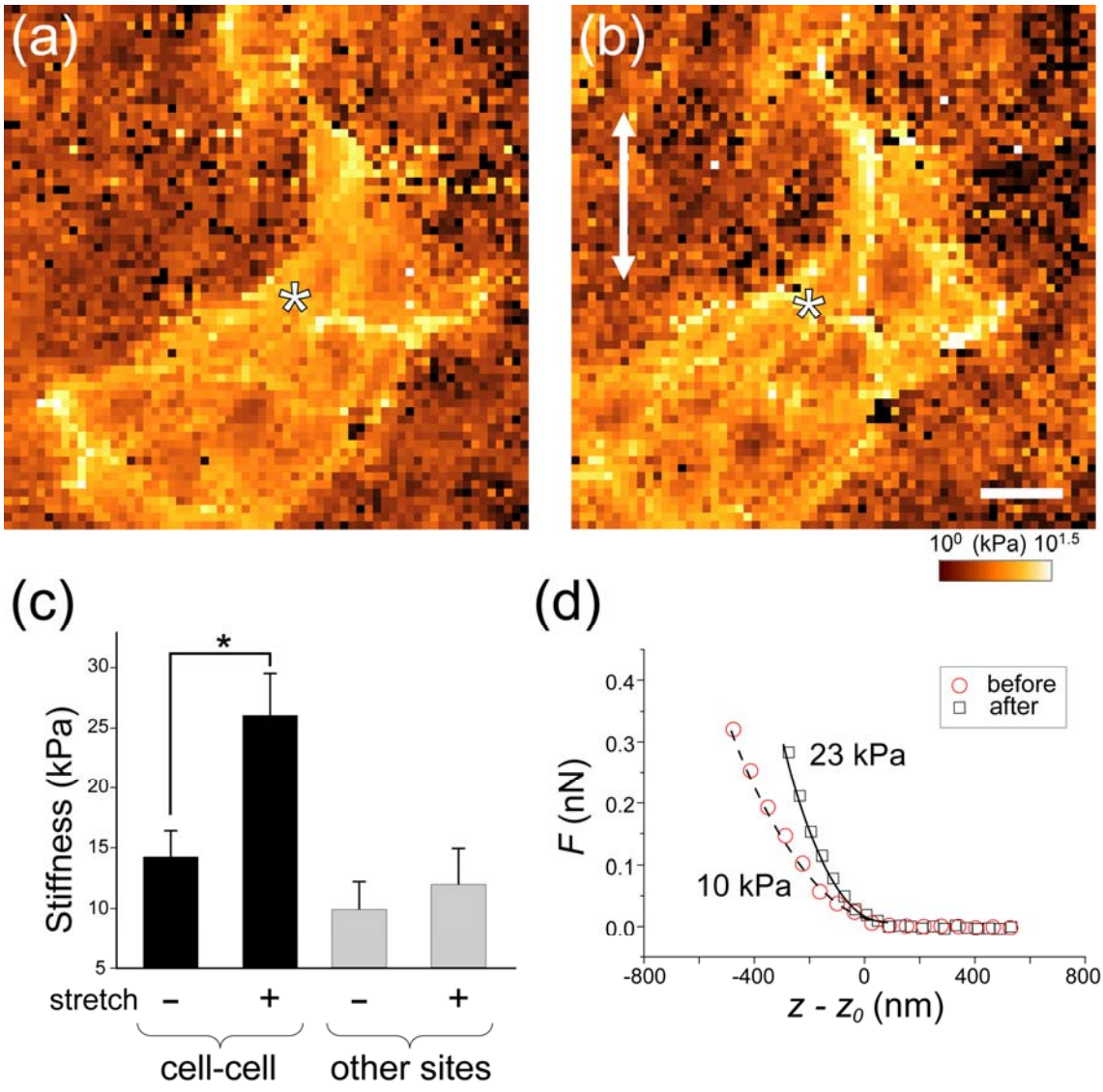

Figure 3

Color figure

Width = 17.7 cm

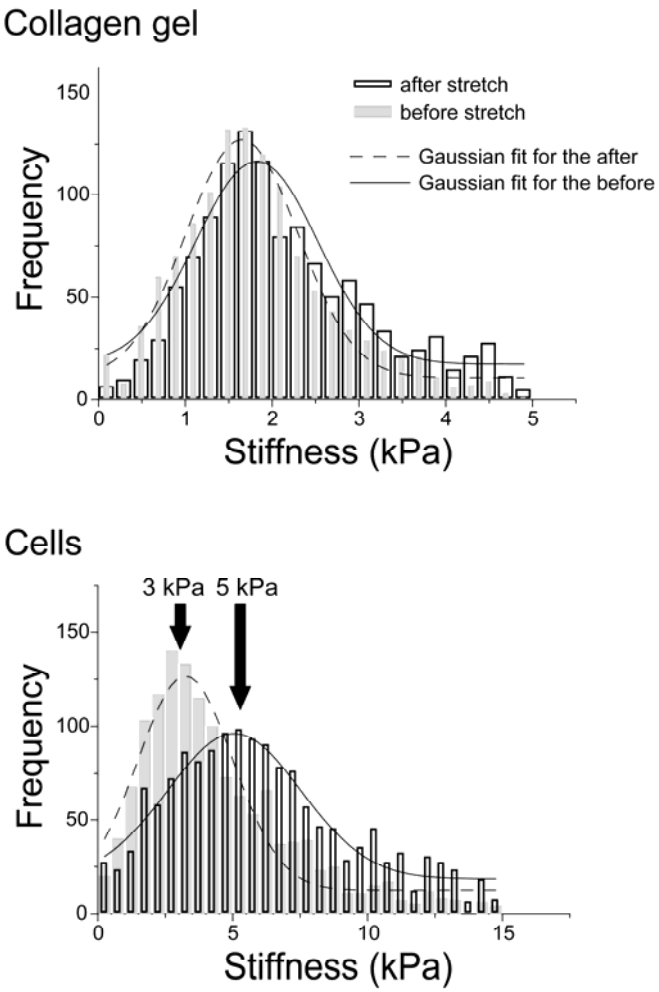

Figure 4

Width = 8.6 cm

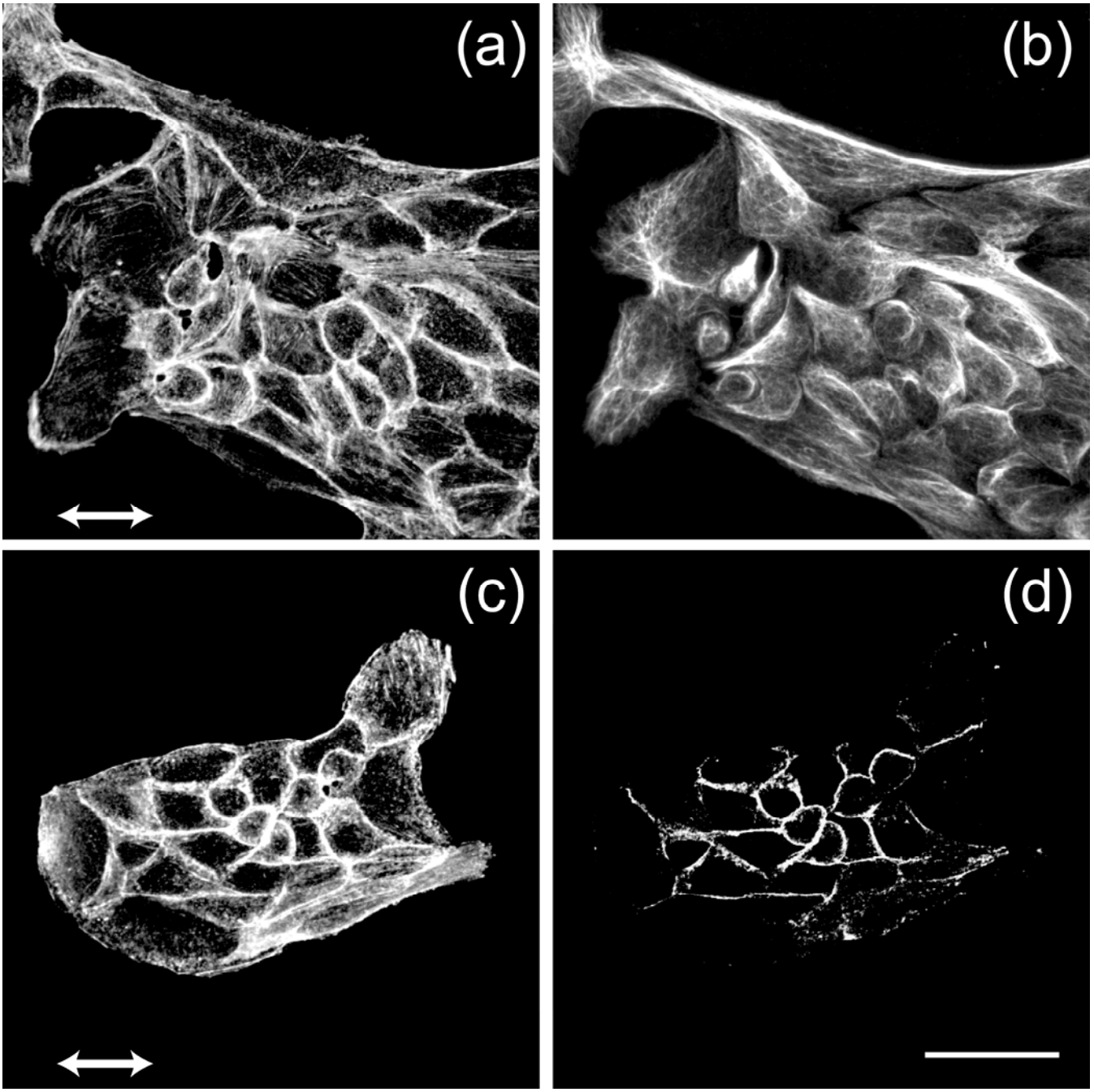

Figure 5

Width = 17.7 cm

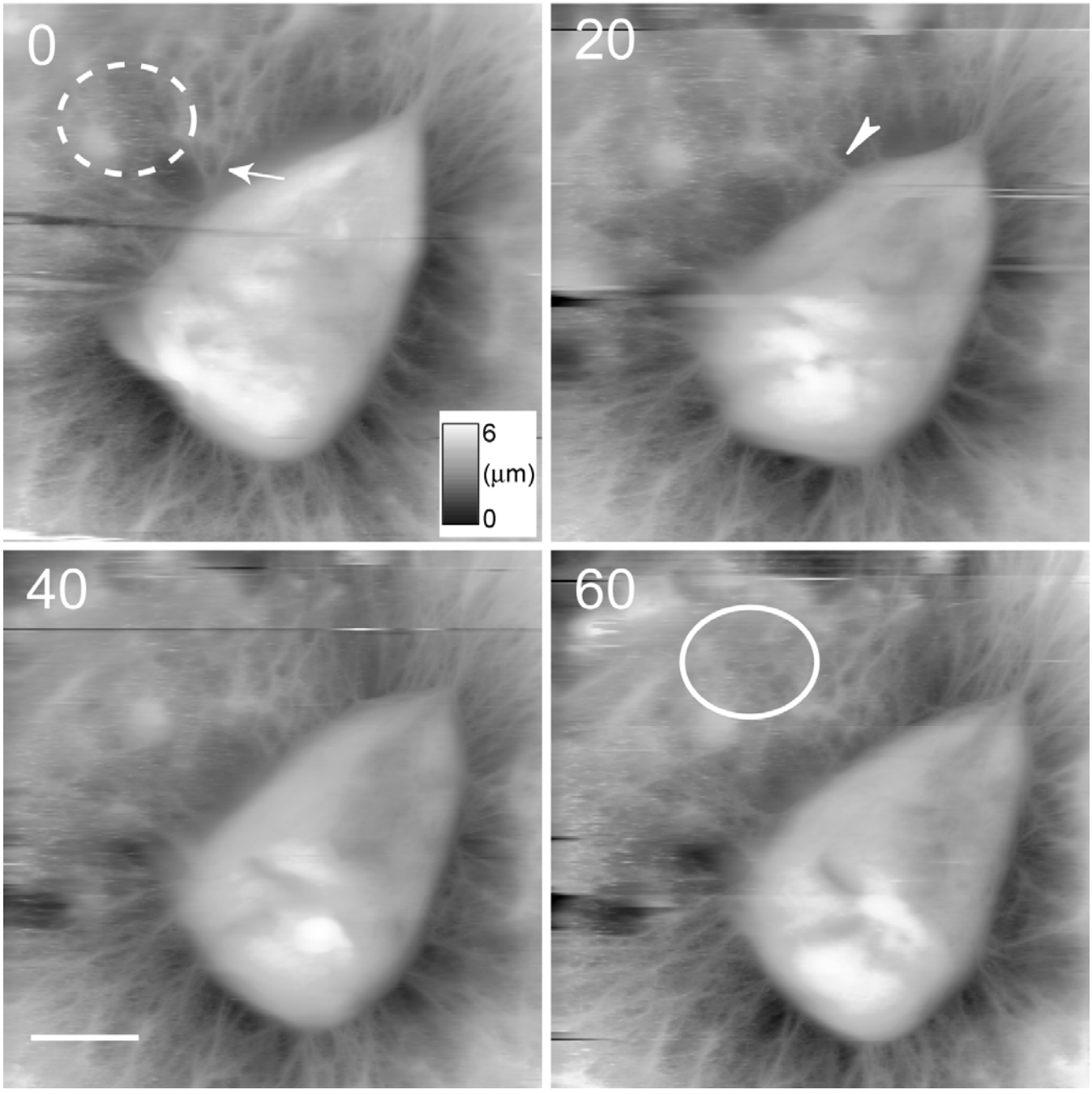

Figure 6

Width = 17.7 cm